A continuous model for connectivity constraints in topology optimization

A. Donoso · E. Aranda · D. Ruiz

Abstract The aim of this work is to present a continuos mathematical model that characterizes and enforces connectivity in a topology optimization problem. That is accomplished by constraining the second eigenvalue of an auxiliary eigenproblem, solved together with the governing state law in each step of the iterative process. Our density-based approach is illustrated with 2d and 3d numerical examples in the context of structural design.

Keywords connectivity · topology optimization · enclosed holes · isolated features

1 Introduction

Connectivity is an important issue in topology optimization (TO) that affects in a different way depending on the physical meaning of the phases involved in the problem. In structural design, for instance, while optimized designs are connected, it is quite often that several enclosed holes appear in minimum compliance structures [1–4]. Those holes are desirable from a stiffness perspective, but lead to a distribution of the void phase which is not connected, and that definitely complicates the fabrication of the final structure.

A. Donoso · E. Aranda
Departamento de Matemáticas, ETSII
Universidad de Castilla - La Mancha
Ciudad Real, Spain

D. Ruiz
Departamento de Matemáticas, EIIA
Universidad de Castilla - La Mancha
Toledo, Spain

A. Donoso (Corresponding Author)
E-mail: Alberto.Donoso@uclm.es

Something similar happens at the nanoscale when tailoring dispersion properties in photonic crystal waveguides (PhCWs). In the case of slow-light 2d structures, the usual is considered a super-cell, to be periodically repeated, made from a dielectric substrate with air-holes. Typically, the design domain occupies a central region in the super-cell. When optimizing the dielectric material distribution, sometimes solid regions appear as free-floating members in the final layouts that are impossible to realize [5, 6]. Additionally, enclosed air-voids appear in the design of 3d band-gap structures. Those pores are advantageous from optimization point of view, but not easy to be manufactured [7–9]. It was precisely in [5] where a technique to avoid the appearance of isolated components in PhCWs was proposed. It was achieved by forcing that the fundamental free mechanical vibration frequency of the super-cell to stay above a given parameter.

Another scenario where lack of connectivity becomes relevant takes place when performing electrode design in piezo modal transducers. Typical electrode patterns correspond to polarization profiles which take on two values only, i.e. either positive or negative polarity, which are the phases here. In general, electrodes hardly ever present profiles of both phases connected, and they typically exhibit isolated features of like-polarity [10, 11], which makes it difficult the wiring schemes.

As far as the authors' knowledge, the first strategy to tackle connectivity in structural design was the virtual temperature method (VTM) [12, 13]. The idea consists in solving an auxiliary linear thermal problem where void/solid are treated as conductive/insulator material, respectively, and some parts of the boundary behave as heat sinks. There, void connectivity is imposed by constraining the maximum temperature in the void phase. VTM was also extended to the molding

constraint [14], and to the electrode connectivity problem in [15] by solving two auxiliary thermal problems, one for each phase. And in [16], VTM was modified by introducing a nonlinear heat source. That improvement lets generate a uniformly distributed temperature field in all regions covered by enclosed voids, so that the temperature threshold value is independent on the problem.

In the last years, other appealing strategies, most of them supported by physical arguments, have been proposed to address the connectivity issue in structural design [16–21]. Furthermore, above reference [9] presents different types of constraints (some of them are extensions of [5] and [12]) for designing topology optimized periodic structures like 3d photonic crystals without isolated components of material or enclosed pores.

Recently, the authors have developed a new method for imposing connectivity constraints which is based on known results of spectral graph theory. It has been successfully applied to structural design [22] and to electrode design [23]. Inspired by those works, we propose here a continuous mathematical model that lets both characterize and enforce connectivity in any of the two phases (or even in both) involved in a topology optimization problem, and more importantly, regardless of the physical situation. Somehow, this approach presents some similarities with the technique used in [5] and the VTM itself, but we lay particular emphasis on the fact that our model rests on mathematical basis from spectral theory.

The paper is organized as follows. Section 2 presents a continuous mathematical model based on the eigenvalues of the Neumann-Laplacian operator that succeeds in detecting whether a phase in a domain where coexisting two phases is connected or not. That can be achieved by solving an appropriate eigenvalue problem. Section 3 provides a TO-formulation that imposes connectivity over the void phase in structural design. Several numerical examples that corroborate our method are included here. Finally, some conclusions and future work are commented in the last section.

2 A model for connectivity

It is known (see [24, Chapter VI, §1.3]) that if ω is a bounded open Lipschitzian set in $\mathbb{R}^N$, the first eigenvalue of the Laplacian operator with Neumann boundary condition, the so-called Neumann-Laplacian, is zero; and if ω is connected, the second eigenvalue is strictly positive. Also if ω is not connected, we obtain its eigenvalues by collecting and reordering the eigenvalues of each connected components. Therefore, the connectivity of a set can be characterized looking at the second

eigenvalue of the Neumann-Laplacian: the set is connected if and only if the second eigenvalue is positive.

Our idea here is to identify the connectivity of a set defined by a density function which is a solution of a minimum compliance problem in TO. Ideally, the solution of such a problem would be a characteristic function of the set where we put the material, but typically what we obtain is a density function $\rho \in [0, 1]$ defined in the reference domain Ω. So, if a sequence of density functions ρ_n converges (pointwise) to a characteristic function χ_ω, we would like to establish a relationship between the second eigenvalue of the Neumann-Laplacian in ω and the limit of the second eigenvalue of the problems

$$\left. \begin{aligned} -\mathrm{div}((\epsilon + (1 - \epsilon)\rho_n)\nabla\phi) &= \lambda\rho_n\phi \ \ \text{in } \Omega, \\ \frac{\partial\phi}{\partial\vec{n}} &= 0 \ \ \text{on } \partial\Omega, \end{aligned} \right\} \qquad (1)$$

where $\epsilon > 0$ is fixed. Notice that we need to include this parameter in order to have a well posed problem.

First, using [25, Theorem 2.3.3] we have the convergence of the eigenvalues of (1) to the eigenvalues of the problem

$$\left. \begin{aligned} -\mathrm{div}((\epsilon + (1 - \epsilon)\chi_\omega)\nabla\phi) &= \lambda\chi_\omega\phi \ \ \text{in } \Omega, \\ \frac{\partial\phi}{\partial\vec{n}} &= 0 \ \ \text{on } \partial\Omega. \end{aligned} \right\} \qquad (2)$$

The following result relates the second eigenvalue of the Neumann-Laplacian in ω with the second eigenvalue of (2):

Theorem 1 *Let μ be the second eigenvalue of the problem*

$$\left. \begin{aligned} -\Delta\phi &= \lambda\phi \ \ in \ \omega, \\ \frac{\partial\phi}{\partial\vec{n}} &= 0 \ \ on \ \partial\omega. \end{aligned} \right\} \qquad (3)$$

If λ denotes the second eigenvalue of (2), then there exists a constant $C > 0$ such that $\lambda - \mu \leq C\epsilon$.

Proof Using the Rayleigh quotient (see [25]), we have the characterization of the second eigenvalue of problem (3):

$$\mu = \min_{\substack{\phi \in H^1(\omega), \\ \int_\omega \phi\, dx = 0}} \frac{\displaystyle\int_\omega |\nabla\phi|^2\, dx}{\displaystyle\int_\omega \phi^2\, dx}.$$

Let ϕ^* such that the minimum is attained,

$$\mu = \frac{\displaystyle\int_\omega |\nabla\phi^*|^2\, dx}{\displaystyle\int_\omega (\phi^*)^2\, dx}, \quad \phi^* \in H^1(\omega), \ \int_\omega \phi^*\, dx = 0.$$

Let we consider an open bounded domain Ω' such that $\Omega \subset\subset \Omega'$. The extension theorem in Sobolev spaces (see [26, §5.3, Theorem 1]) guarantees the existence of $u^* \in H^1(\mathbb{R}^N)$ such that $u^* = \phi^*$ in ω and u^* has support in Ω'. This extension also satisfies

$$\|u^*\|_{H^1(\mathbb{R}^N)} \le \tilde{C}\|\phi^*\|_{H^1(\omega)}. \tag{4}$$

Now, we define $u = u^* - \alpha$, where $\alpha = \frac{1}{|\Omega|}\int_\Omega u^*\,dx$. Then $u \in H^1(\Omega)$ with zero mean value, and therefore

$$\begin{aligned}
\lambda &= \min_{\substack{v \in H^1(\Omega), \\ \int_\Omega v\,dx=0}} \frac{\int_\Omega ((1-\epsilon)\chi_\omega + \epsilon)\,|\nabla v|^2\,dx}{\int_\Omega \chi_\omega v^2\,dx} \\
&\le \frac{\int_\Omega ((1-\epsilon)\chi_\omega + \epsilon)\,|\nabla u|^2\,dx}{\int_\Omega \chi_\omega u^2\,dx} \\
&= \frac{(1-\epsilon)\int_\omega |\nabla u|^2\,dx + \epsilon\int_\omega |\nabla u|^2\,dx + \epsilon\int_{\Omega\setminus\omega} |\nabla u|^2\,dx}{\int_\omega u^2\,dx}
\end{aligned} \tag{5}$$

Notice that, as $u^* = \phi^*$ in ω then $\nabla u^* = \nabla \phi^*$ in ω, and, it is clear that $\nabla u = \nabla u^*$, so the first two terms in the numerator of (5) are equal to $\int_\omega |\nabla\phi^*|^2\,dx$.

The third term in this numerator

$$\int_{\Omega\setminus\omega} |\nabla u|^2\,dx \le \int_{\Omega'} |\nabla u^*|^2\,dx \le \|u^*\|^2_{H^1(\mathbb{R}^N)}$$

and using (4)

$$\int_{\Omega\setminus\omega} |\nabla u|^2\,dx \le \tilde{C}^2\|\phi^*\|^2_{H^1(\omega)}.$$

On the other hand, we can bound the denominator of (5):

$$\begin{aligned}
\int_\omega u^2\,dx &= \int_\omega (u^* - \alpha)^2\,dx \\
&= \int_\omega (u^*)^2\,dx + \alpha^2|\omega| - 2\alpha\int_\omega u^*\,dx \\
&= \int_\omega (\phi^*)^2\,dx + \alpha^2|\omega| \ge \int_\omega (\phi^*)^2\,dx,
\end{aligned}$$

(remember that $u^* = \phi^*$ in ω). So finally, substituting at (5)

$$\lambda \le \frac{\int_\omega |\nabla\phi^*|^2\,dx + \epsilon\tilde{C}^2\|\phi^*\|^2_{H^1(\omega)}}{\int_\omega (\phi^*)^2\,dx} = \mu + C\epsilon.$$

This finishes the proof. □

This result guarantees that the second eigenvalue of a domain ω and the second eigenvalue of problem (2) are closed enough, what can be used to capture the connectivity of a domain.

It is quite common to introduce a shifting method in the eigenvalues' computation, so we will change λ by $\lambda - 1$ in problems (1)–(3), and instead of looking at 0 eigenvalue, we will focus on 1 eigenvalue.

As an example, let us consider Ω be the unit square, and ω the subset defined by the two black rectangles of Figure 1. The exact eigenvalues of (3) are known,[1] and the first five (with shifting) correspond to 1, 1, $1 + \pi^2$, $1 + 4\pi^2$, $1 + \frac{\pi^2}{(0.4)^2}$. Note that there are two eigenvalues equal to 1 because ω is not connected. Table 1 shows the numerical approximation of shifted problem (2) for different values of ϵ, where a finite element (FE) discretization over two different meshes (100×100 and 200×200) have been considered.
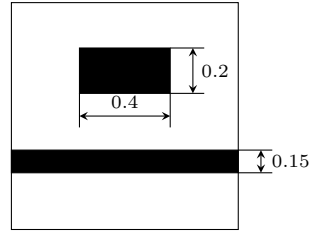

Fig. 1 Ω (unit square) and ω (two black rectangles).

While the first eigenvalues are always 1, the second eigenvalues are strictly greater than 1 because of problem (2) is set in Ω, which is connected. However, we can see that, for small ϵ, the second eigenvalues are closed to 1, son we can derive from here that ω is not connected.

However, problem (2) is an ideal situation. In practise, what we have is a problem like (1), with a density ρ with intermediate values between 0 and 1. So, in the same spirit as the SIMP (Solid Isotropic Method with Penalization) does, we introduce the problem

$$\left.\begin{aligned}
-\operatorname{div}(w(\rho)\nabla\phi) &= (\lambda - 1)\rho\phi \ \text{ in } \Omega, \\
\frac{\partial\phi}{\partial n} &= 0 \ \text{ on } \partial\Omega,
\end{aligned}\right\} \tag{6}$$

where

$$w(\rho) = (1-\epsilon)\rho^r + \epsilon,$$

and r is a power that penalizes intermediate densities.

---

[1] The eigenvalues of the Neumann-Laplacian for a rectangle $(0, L) \times (0, l)$ without shifting are $\mu_{m,n} = \pi^2\left(\frac{m^2}{L^2} + \frac{n^2}{l^2}\right)$, $m, n \ge 0$.

	$\epsilon = 10^{-3}$	$\epsilon = 10^{-5}$	$\epsilon = 10^{-7}$	$\epsilon = 10^{-9}$	Exact
λ_2	1.0736276916	1.0007367590	1.0000073676	1.0000000736	1.000
	1.0735863857	*1.0007363432*	*1.0000073634*	*1.0000000736*	
λ_3	10.9107576249	10.8708198860	10.8704202074	10.8704162105	10.8696044010
	10.9101331588	*10.8702108966*	*10.8698113739*	*10.8698073787*	
λ_4	40.5748127523	40.4922414054	40.4914155337	40.4914072750	40.4784176043
	40.5650486484	*40.4824986791*	*40.4816730208*	*40.4816647642*	
λ_5	62.8431902703	62.7180075845	62.7167553598	62.7167428375	62.6850275068
	62.8192328609	*62.6942182563*	*62.6929677180*	*62.6929552126*	

Table 1 Numerical eigenvalues of problem (2) for different values of ϵ with meshes 100×100 (upright font) and 200×200 (*slanted font*).

So, the idea of our method relies on imposing that the second eigenvalue of (6) must be strictly greater than 1. Therefore, if ρ is closed to a characteristic function of some subset ω, then ω has to be connected. In some way, a high value of r introduces an additional requirement for connectivity which favours convergence, but at the same time the rest of eigenvalues are distorted.

Table 2 shows the numerical results for problem (6) with different values of r, where ρ is a density obtained by filtering (with the usual conic filter of radius 0.03) the characteristic function χ_ω of Figure 1. Note that the second eigenvalue still detects the no connectivity of ω.

	$r = 1$	$r = 3$	$r = 6$	$r = 12$	Exact
λ_2	1.0009	1.0009	1.0008	1.0007	1.0000
λ_3	10.8709	9.6161	4.2232	1.5346	10.8696
λ_4	40.4924	35.3811	4.2415	1.5358	40.4784
λ_5	62.6677	56.0582	4.2500	1.5444	62.6850

Table 2 Eigenvalues for problem (6) for a non binary density, with different values of r in a 100×100 mesh and $\epsilon = 10^{-5}$.

## 3 Optimal design without internal voids

The classical compliance minimization problem in topology optimization leads to connected designs because of physical considerations: forces need to be propagated along the structure and isolated features of material do not contribute to increase stiffness. At the same time, the stiffness requirement typically results in the formation of several enclosed holes that can complicate the fabrication of the final design (specially for 3d problems). Those internal holes in an structure can be seen as different connected components of the set where we do not put the material, or in terms of the density function ρ, the set where $\rho = 0$. Therefore, a simple way to avoid the formation of internal holes is imposing the connectivity of that set, or, in terms of the eigenvalue problem (6), forcing that the second eigenvalue

be strictly greater than 1, where

$$w(\rho) = (1 - \epsilon)(1 - \rho)^r + \epsilon. \qquad (7)$$

Notice that we have changed ρ by $1 - \rho$ as we are now focused on the connectivity of the void phase.

However, it is still possible to have a disconnected void phase without any internal hole, as we can see at Figure 1, where there are no internal holes in the structure, but void phase is not connected. This situation can be easily avoided if we consider a frame around Ω where $\rho = 0$. We denote by $\Omega^\sharp$ to this extended domain (see Figure 2), and still denote by ρ the extension of ρ by null values outside of Ω. Now, it is clear that the number of enclosed holes are equal to the number of connected components of the void phase minus one. So having no internal holes is equivalent to a connected void phase in $\Omega^\sharp$.
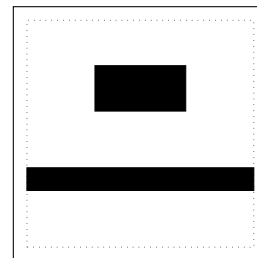
Fig. 2 Ω (dotted line) and the extended domain $\Omega^\sharp$. Void phase is now connected.

Therefore, discretizing (6) by FE leads to consider the discrete problem

$$\begin{cases} (\mathcal{K}(\boldsymbol{\rho}) - (\lambda_2 - 1)\mathcal{M}(\boldsymbol{\rho})) \, \boldsymbol{\Phi}_2 = \mathbf{0} \\ \boldsymbol{\Phi}_2^T \mathcal{M}(\boldsymbol{\rho}) \boldsymbol{\Phi}_2 = 1 \end{cases} \qquad (8)$$

where $\mathcal{K}$ and $\mathcal{M}$ are the global stiffness and mass matrices, respectively, $\boldsymbol{\rho}$ corresponds to the vector of discretized densities in the extended domain (extended with null values), and $(\lambda_2, \boldsymbol{\Phi}_2)$ is the pair eigenvalue and its associated $\mathcal{M}$-orthonormal eigenvector, respectively.

Table 3 shows, in an example of a real minimum compliance structure, how internal holes are detected and compare the effect of considering or not the extended domain (a small outside frame of void phase of three elements size). In this case, three isolated void areas are identified in the structure delimited by the dashed-line (i.e., without void frame), but they collapse in only two when considering the void frame. Here, as in the rest of numerical experiments that will appear below we have used $r = 12$ and $\epsilon = 10^{-5}$.

	Void without frame	Void with frame	
λ_1	1	1	
λ_2	1.0005	1.0028	
λ_3	1.0011	1.3085	
λ_4	1.2154	1.4103	

Table 3 The first four eigenvalues for the problem (8) for the white phase (void)

It is worth mentioning that discrete approach (8) somehow reminds us the one developed by the authors in [22] based on spectral graph theory. In fact, that previous work has definitely inspired us for developing the continuous mathematical model proposed here for characterizing void connectivity. Consequently, it gives us the key to enforce connectivity constraints in TO-problems: that is, imposing that $\lambda_2 > 1$ in $\Omega^\sharp$.

4 Formulation and numerical examples

Having in mind the considerations of the previous section, the problem formulation for minimum compliance that incorporates void-phase connectivity may be written as

$$\min_{\boldsymbol{\rho} \in [0,1]} \mathbf{F}^T \mathbf{U}$$
$$\text{s.t.} \begin{cases} \mathbf{v}^T \hat{\boldsymbol{\rho}}_E \leq V_0 |\Omega|, \\ \lambda_2 > 1, \end{cases}$$

where $\mathbf{F}$ are the external force vectors and $\mathbf{U}$ are the global displacements, so that the objective function is the usual compliance. $\mathbf{U}$ is obtained solving the (discrete) elasticity system

$$\mathbf{K}(\hat{\boldsymbol{\rho}}_E)\mathbf{U} = \mathbf{F}, \qquad (9)$$

and $\mathbf{K}$ is the global stiffness matrix. The first constraint corresponds to the volume constraint, where $\mathbf{v}$ is a vector containing the measure of the elements, V_0 is the (given) volume fraction and $|\Omega|$ is the measure of the

design domain. And the second constraint corresponds to the second eigenvalue of the problem

$$\begin{cases} \left(\mathcal{K}(\hat{\boldsymbol{\rho}}_C) - (\lambda_2 - 1)\mathcal{M}(\hat{\boldsymbol{\rho}}_C)\right)\boldsymbol{\Phi}_2 = \mathbf{0} \\ \boldsymbol{\Phi}_2^T \mathcal{M}(\hat{\boldsymbol{\rho}}_C)\boldsymbol{\Phi}_2 = 1 \end{cases} \qquad (10)$$

that is, the void connectivity constraint.

As usual in TO, the density is filtered with a typical conic filter and then projected with a smoothed Heaviside function. We have use the one proposed in [27]

$$P_\beta(\rho_e) = e^{-\beta(1-\rho_e)} - (1-\rho_e)e^{-\beta},$$

but we have considered different proyections for each subproblem. While for the elasticity problem and volume constraint, the values of β are gradually increased as usual to force 0/1 designs, the strategy for the computation of eigenvalues in (10) is to fix $\beta = 8$ from the beginning in order to better identify holes. This is why we have different notations for the filtered and proyection densities: $\hat{\boldsymbol{\rho}}_E$ is the density used in the computation of (9) and volume constraint, and $\hat{\boldsymbol{\rho}}_C$ is the density used in (10), which has been previously extended to the domain $\Omega^\sharp$.

With regard to the sensitivity analysis, it just requires special mention the derivative of an eigenvalue, something that is well-known, given by

$$\frac{\partial \lambda_2}{\partial \rho_e} = \boldsymbol{\Phi}_2^T \left(\frac{\partial \mathcal{K}}{\partial \rho_e} - (\lambda_2 - 1)\frac{\partial \mathcal{M}}{\partial \rho_e} \right) \boldsymbol{\Phi}_2.$$

Note that $\rho_e = 0$ on the elements of the extension, so the partial derivatives do not change.

A continuation strategy has been implemented in the connectivity constraint, beginning with $\lambda_2 > 1.05$ and ending with $\lambda_2 > 1.15$, increasing the value of the eigenvalue in 0.01 for each 50 iterations.

Two examples in 2d, a cantilevered beam with a load applied in the middle point and a supported bridge with a vertical load in the middle point as well, are used to initially corroborate our method. Optimized structures in both case studies with inner holes and without them are depicted in Fig. 3 and Fig. 4, respectively. A more interesting example takes place in 3d, previously studied in [21]. There, a platform type-structure with null displacements in the red region of the bottom surface is subject to uniform pressure on the top surface. A quarter structure discretized into $40 \times 40 \times 30$ elements is simulated by symmetry. Three layers of elements on the top of the structure are chosen as a non-design domain. Optimized designs with and without connectivity constraints for $V_0 = 0.3$ are showed in Fig. 5.

(a)

(b)
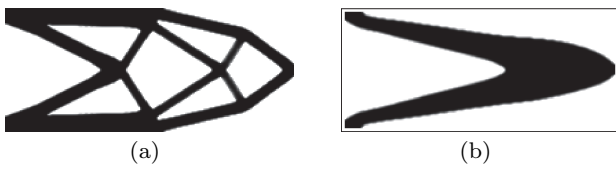
Fig. 3 Example of a cantilevered beam with a load in the middle point. (a) minimum compliance design; (b) the same but forcing that void phase to be connected in the extended domain.

(a)

(b)
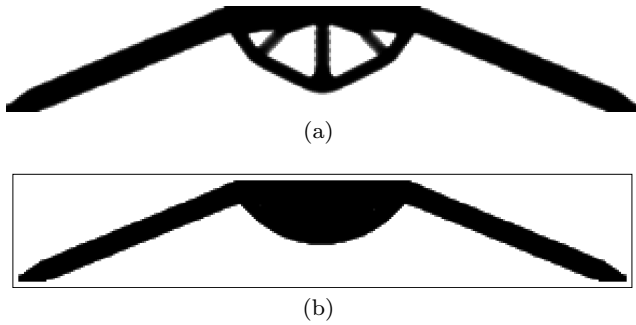
Fig. 4 Example of a supported bridge with a load in the middle point. (a) minimum compliance design; (b) the same but forcing that void phase to be connected in the extended domain.

5 Final remarks

This work proposes a continuous model that imposes void connectivity in structural design, thus avoiding the formation of inner holes in topology optimized structures. The idea behind the method can be used to enforce connectivity in other physical contexts of interest in a straightforward manner, and we plan to explore it in a near future.
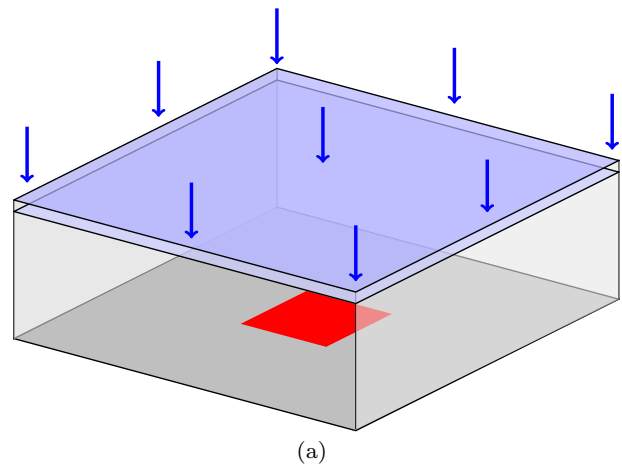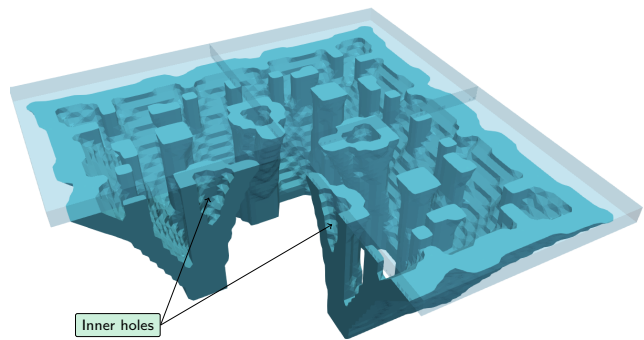
Conflict of interest

On behalf of all authors, the corresponding author states that there is no conflict of interest.
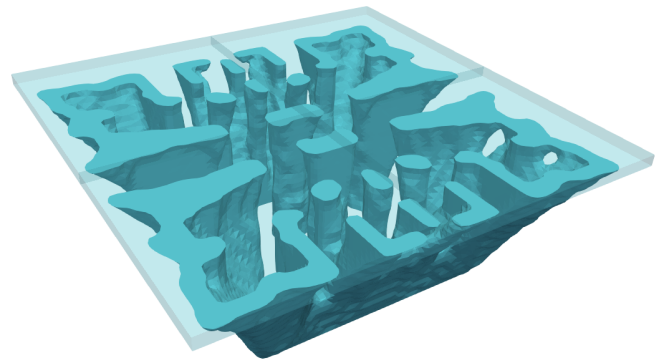
Replication of results

The authors honestly believe that all information needed to reproduce above results has been provided.

(a)

Inner holes

(b)

(c)

Fig. 5 Example of a minimum compliance platform. (a) design domain and boundary conditions; (b) optimized structure without connectivity constraints; (c) the same with connectivity constraints.

References

1. O. Sigmund, On the optimality of bone microstructure, in: P. Pedersen, M. P. Bendsøe (Eds.), IUTAM Symposium on Synthesis in Bio Solid Mechanics, Springer Netherlands, Dordrecht, 2002, pp. 221–234.
2. V. J. Challis, J. K. Guest, J. F. Grotowski, A. P. Roberts, Computationally generated cross-property bounds for

stiffness and fluid permeability using topology optimization, International Journal of Solids and Structures 49 (23) (2012) 3397 – 3408.

3. O. Sigmund, N. Aage, E. Andreassen, On the (non-)optimality of michell structures, Structural and Multidisciplinary Optimization 54 (2) (2016) 361–373.

4. M. Osanov, J. K. Guest, Topology optimization for architected materials design, Annual Review of Materials Research 46 (1) (2016) 211–233.

5. F. Wang, J. S. Jensen, O. Sigmund, Robust topology optimization of photonic crystal waveguides with tailored dispersion properties, J. Opt. Soc. Am. B 28 (3) (2011) 387–397.

6. R. E. Christiansen, O. Sigmund, Inverse design in photonics by topology optimization: tutorial, J. Opt. Soc. Am. B 38 (2) (2021) 496–509.

7. H. Men, K. Y. K. Lee, R. M. Freund, J. Peraire, S. G. Johnson, Robust topology optimization of three-dimensional photonic-crystal band-gap structures, Opt. Express 22 (19) (2014) 22632–22648.

8. K. E. Swartz, D. A. White, D. A. Tortorelli, K. A. James, Topology optimization of 3d photonic crystals with complete bandgaps, Opt. Express 29 (14) (2021) 22170–22191.

9. K. E. Swartz, D. A. Tortorelli, D. A. White, K. A. James, Manufacturing and stiffness constraints for topology optimized periodic structures, Struct Multidisc Optim 65 (129) (2022).

10. D. Ruiz, J. Bellido, A. Donoso, Optimal design of piezoelectric modal transducers, Arch Computat Methods Eng (25) (2018) 313–347.

11. A. Donoso, J. C. Bellido, Robust design of multimodal piezoelectric transducers, Comput Methods Appl Mech Engrg 338 (2018) 27–40.

12. S. Liu, Q. Li, W. Chen, L. Tong, G. Cheng, An identification method for enclosed voids restriction in manufacturability design for additive manufacturing structures, Front Mech Eng 10 (2) (2015) 126–137.

13. M. Osanov, J. Carstensen, E. Tromme, J. Guest, C. Williams, Topology optimization for additive manufacturing: New projection-based design algorithms, in: Proceedings of 17th AIAA/ISSMO Multidisciplinary Analysis and Optimization Conference, Aviation 2016, AIAA, Washington D.C., 2016, pp. 1–9.

14. Q. Li, W. Chen, S. Liu, H. Fan, Topology optimization design of cast parts based on virtual temperature method, Computer-Aided Design 94 (2018) 28–40.

15. A. Donoso, J. K. Guest, Topology optimization of piezo modal transducers considering electrode connectivity constraints, Computer Methods in Applied Mechanics and Engineering 356 (2019) 101–115.

16. Y. Luo, O. Sigmund, Q. Li, S. Liu, Additive manufacturing oriented topology optimization of structures with self-supported enclosed voids, Computer Methods in Applied Mechanics and Engineering 372 (2020) 113385.

17. L. Zhou, W. Zhang, Topology optimization method with elimination of enclosed voids, Struct Multidisc Optim 60 (2019) 117–136.

18. C. Wang, B. Xu, Q. Meng, J. Rong, Y. Zhao, Numerical performance of poisson method for restricting enclosed voids in topology optimization, Computers & Structures 239 (2020) 106337.

19. A. T. Gaynor, T. E. Johnson, Eliminating occluded voids in additive manufacturing design via a projection-based topology optimization scheme, Additive Manufacturing 33 (2020) 101149.

20. G. Sabiston, I. Kim, Void region restriction for additive manufacturing via a diffusion physics approach, Int J Numer Methods Eng 121 (2020) 4347–4373.

21. Y. Xiong, S. Yao, Z.-L. Zhao, Y. M. Xie, A new approach to eliminating enclosed voids in topology optimization for additive manufacturing, Additive Manufacturing 32 (2020) 101006.

22. A. Donoso, E. Aranda, D. Ruiz, A new approach based on spectral graph theory to avoiding enclosed holes in topology optimization, Comput Methods Appl Mech Engrg 393 (2022) 114769.

23. A. Donoso, E. Aranda, D. Ruiz, A new method for designing piezo transducers with connected two-phase electrode, (submitted).

24. R. Courant, D. Hilbert, Methods of mathematical physics. Vol. I. (Translated and revised from the German original.) First English ed, New York: Interscience Publishers xv, 561 p. (1953). (1953).

25. A. Henrot, Extremum Problems for Eigenvalues of Elliptic Operators, Birkhäuser Verlag, Basel - Boston - Berlin, 2006.

26. L. C. Evans, Partial differential equations, 2nd Edition, Vol. 19 of Grad. Stud. Math., Providence, RI: American Mathematical Society (AMS), 2010.

27. O. Sigmund, Morphology-based black and white filters for topology optimization, Struct Multidisc Optim 33 (4-5) (2007) 401–424.